LBL-28330

Lawrence Berkeley Laboratory
UNIVERSITY OF CALIFORNIA

EARTH SCIENCES DIVISION

To be presented at the International High Level
Radioactive Waste Management Conference,
Las Vegas, NV, April 8–12, 1990, and
to be published in the Proceedings

Hydrologic Characterization of Faults and Other Potentially Conductive Geologic Features in the Unsaturated Zone

I. Javandel and C. Shan

January 1990

Prepared for the U.S. Department of Energy under Contract Number DE-AC03-76SF00098.

LOAN COPY
Circulates
for 2 weeks
Bldg. 50 Library.
Copy 2
LBL-28330

DISCLAIMER

This document was prepared as an account of work sponsored by the United States Government. While this document is believed to contain correct information, neither the United States Government nor any agency thereof, nor the Regents of the University of California, nor any of their employees, makes any warranty, express or implied, or assumes any legal responsibility for the accuracy, completeness, or usefulness of any information, apparatus, product, or process disclosed, or represents that its use would not infringe privately owned rights. Reference herein to any specific commercial product, process, or service by its trade name, trademark, manufacturer, or otherwise, does not necessarily constitute or imply its endorsement, recommendation, or favoring by the United States Government or any agency thereof, or the Regents of the University of California. The views and opinions of authors expressed herein do not necessarily state or reflect those of the United States Government or any agency thereof or the Regents of the University of California.

LBL-28330

Hydrologic Characterization of Faults and Other Potentially Conductive Geologic Features in the Unsaturated Zone

I. Javandel and C. Shan

Earth Sciences Division
Lawrence Berkeley Laboratory
University of California
Berkeley, California 94720

January 1990

This work was supported by the Director, Office of Civilian Radioactive Waste Management, Office of Facilities Siting and Development, Siting and Facilities Technology Division, of the U.S. Department of Energy under Contract No. DE-AC03-76SF00098.

HYDROLOGIC CHARACTERIZATION OF FAULTS AND OTHER POTENTIALLY CONDUCTIVE GEOLOGIC FEATURES IN THE UNSATURATED ZONE

IRAJ JAVANDEL and CHAO SHAN
Earth Sciences Division
Lawrence Berkeley Laboratory
University of California
Berkeley, California 94720
(415) 486-6106

ABSTRACT

The capability of characterizing near-vertical faults and other potentially highly conductive geologic features in the vicinity of a high-level-waste repository is of great importance in site characterization of underground waste-isolation projects. The possibility of using transient air pressure data at depth (resulting from surface barometric pressure fluctuations) for characterizing these features in the unsaturated zone are investigated. Analytical solutions for calculating the pressure response of such systems are presented. Solutions are given for two types of barometric pressure fluctuations, step function and sinusoidal.

INTRODUCTION

The capability of characterizing near-vertical faults and other potentially highly conductive geologic features in the vicinity of a high-level-waste repository is of great importance in underground waste-isolation site characterization projects. The existence of such features near a repository may provide a short travel time flow path from the disturbed zone to the accessible environment.

Measurement of air pressure changes at depth due to atmospheric pressure fluctuations have been used before to estimate the permeability of geologic strata .[1] In those studies the assumption was made that no open borehole, fractures, or other geologic structures exist that would provide preferred flow paths for air movement. When a conductive fault cuts through layers of geologic materials with lower permeability, points located in the fault zone will experience pressure variations faster and more pronounced than points in the rock mass located at the same elevation. It is desirable to obtain a solution that allows the calculation of pressure response due to the atmospheric pressure variations in a multilayer geologic system with a cross-cutting highly-conductive fault. As a first step, we have developed a series of analytical solutions to calculate the propagation of atmospheric pressure changes in a single-layer system that is intersected by a vertical fault or other planar conductive features. Comparison of pneumatic pressure variations between the fault zone and the surrounding rock mass could provide a means for estimating the permeability of the fault zone.

In this paper we shall present two of these new analytical solutions. These solutions, though limited in application for multilayered geologic systems, could be used for verification of numerical codes that could then be extended to multilayered media.

MATHEMATICAL MODELS

Let us consider a single horizontal geologic layer that is cut by a vertical fault zone with a thickness of $2b'$, as shown in Figure 1. We would like to derive solutions to calculate air pressure changes due to atmospheric pressure fluctuations, as a function of time and position within the system.

The medium is extensive both horizontally and vertically such that mathematically it could be assumed to be infinite in both directions. Since the mid-plane of the fault zone is a symmetry plane, only half of the system will be considered in the analysis. A Cartesian coordinate system is selected such that its origin is at the intersection of the ground surface with the contact plane between the fault and the rock mass. The x-axis is horizontal and perpendicular to the rock-fault zone interface, and the z-axis is oriented vertically downwards.

The partial differential equations governing the isothermal flow of air in the unsaturated porous media may be written as[1] :

$$\frac{\partial^2\phi'^2}{\partial x'^2} + \frac{\partial^2\phi'^2}{\partial z'^2} = \frac{\mu_a n_a}{k'\bar{p}} \cdot \frac{\partial\phi'^2}{\partial t'} \qquad (1)$$

where

$\phi' = \frac{p}{\rho_a g} - z'$ = pneumatic head, L;

$\bar{p}$ = mean pressure of the system, M/LT^2;

μ_a = viscosity of air, M/LT;

n_a = interconnected air-filled porosity at the prevailing moisture content;

k' = air permeability of the medium at the prevailing moisture content, L^2;

t' = time, T.

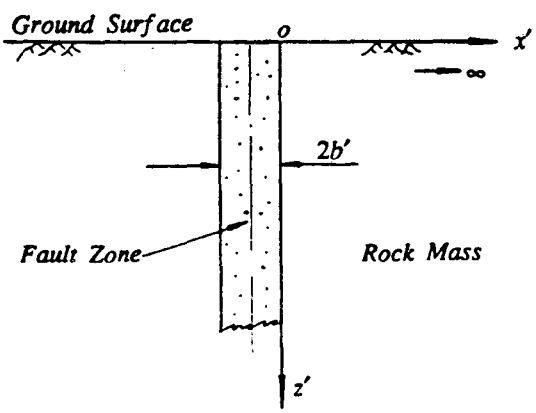

Figure 1. Schematic cross section of the fault zone and surounding rocks.

Assumptions inherent in the development of Equation (1) are as follows:

- the medium is homogeneous and isotropic with a constant moisture content;
- air permeability of the medium is large enough that the Klinkenberg[2] effect is negligible;
- absolute pressure is small enough that the ideal gas laws apply;
- the change in pressure with depth has a negligible effect on air density.

In this study, similar to that of Weeks[1], we have assumed that pneumatic head varies only slightly from its mean value. Under this condition, Equation (1) may be approximated to the following form that is linear with respect to ϕ'.

$$\frac{\partial^2\phi'}{\partial x'^2} + \frac{\partial^2\phi'}{\partial z'^2} = \frac{1}{\alpha'}\cdot\frac{\partial\phi'}{\partial t'} \tag{2}$$

where $\alpha' = \frac{k'\bar{p}}{\mu_a n_a}$ is pneumatic diffusivity.

Furthermore, flow in the fault zone is assumed to be one-dimensional in the vertical direction, while the flux crossing the fault-rock interface is treated as a sink term in the governing equation for the fault zone. The impact of some of the above assumptions will be discussed later in the paper. Based on the above assumptions, the mathematical model for the system under consideration may be written as follows.

In a dimensionless form, the partial differential equations for the intact rock and the fault zone are:

$$\frac{\partial^2\phi_r}{\partial x^2} + \frac{\partial^2\phi_r}{\partial z^2} = \frac{1}{\alpha}\cdot\frac{\partial\phi_r}{\partial t} \tag{3}$$

$$\frac{\partial^2\phi_f}{\partial z^2} + k\left(\frac{\partial\phi_r}{\partial x}\right)_{x=0} = \frac{\partial\phi_f}{\partial t} \tag{4}$$

where the subscripts 'r' and 'f' refer to the intact rock and the fault zone, respectively. Dimensionless terms applied in the formulations are defined as,

$$x = \frac{x'}{b'} \qquad z = \frac{z'}{b'} \qquad k = \frac{k'_r}{k'_f}$$

$$\phi = \frac{\phi' - \phi'_0}{\phi'_b - \phi'_0} \qquad t = \frac{\alpha'_f t'}{b'^2} \qquad \alpha = \frac{\alpha'_r}{\alpha'_f} \tag{5}$$

where ϕ'_0 and ϕ'_b refer to the initial and upper boundary values of the pneumatic head.

As noted above, two types of boundary conditions have been considered for the variation of atmospheric pressure at the ground surface. Type one refers to a step function, and type two to sinusoidal pressure variations.

Except for the boundary conditions at the ground surface, the rest of boundary and initial conditions for both cases are the same, and may be written as,

$$\phi_r(x, z, 0) = \phi_f(z, 0) = 0 \tag{6}$$

$$\phi_r(\infty, z, t) = \text{finite} \tag{7}$$

$$\phi_r(x, \infty, t) = \phi_f(\infty, t) = 0 \tag{8}$$

$$\phi_r(0, z, t) = \phi_f(z, t) \tag{9}$$

Type one boundary condition at the ground surface in non-dimensional form translates to:

$$\phi_r(x, 0, t) = \phi_f(0, t) = 1 \tag{10}$$

For the second type boundary condition, to simplify derivations, one may introduce a new definition for dimensionless pneumatic head as,

$$\phi = \frac{\phi' - \phi'_0}{\phi'_a} \tag{11}$$

where ϕ'_a is the amplitude of pressure head variation, $p_a/\rho_a g$. Now, the second type boundary condition may be written as,

$$\phi_r(x, 0, t) = \phi_f(0, t) = \sin(\omega t) \tag{12}$$

SOLUTIONS

Case 1: Step function atmospheric pressure variation.

Using Laplace transformation with respect to t and Fourier sine transformation with respect to z consecutively, Equations (3) and (4) may be reduced to:

$$\frac{d^2 w_r}{dx^2} - \left(\frac{s}{\alpha} + \rho^2\right) w_r = -\frac{\rho}{s} \tag{13}$$

$$w_f = \frac{1}{s+\rho^2}\left[\frac{\rho}{s} + k\left(\frac{dw_r}{dx}\right)_{x=0}\right] \tag{14}$$

where s and ρ are Laplace and Fourier sine transform parameters, respectively.

The initial condition (6) and boundary conditions (8) and (10) have already been used in deriving Equations (13) and (14).

Equation (13) is a nonhomogeneous second order-ordinary differential equation whose solution satisfying boundary condition (7) may be written as:

$$w_r = C_1 e^{-\sqrt{\frac{s}{\alpha}+\rho^2}\,x} + \frac{\rho}{s\left(\frac{s}{\alpha}+\rho^2\right)} \tag{15}$$

where,

$$C_1 = \left(\frac{1}{\alpha} - 1\right)\cdot\frac{\rho}{\left(\frac{s}{\alpha}+\rho^2\right)\left(s+\rho^2+k\sqrt{\frac{s}{\alpha}+\rho^2}\right)} \tag{16}$$

In evaluating constant C_1 boundary condition (9) has been used. Inversion of Equation (15) to the (x, z, t) domain is lengthy and beyond the scope of this paper. The final solution, however, is given by:

$$\phi_r(x,z,t) = \mathrm{erfc}\left(\frac{z}{2\sqrt{\alpha t}}\right) + \mathrm{erfc}\left(\frac{x}{2\sqrt{\alpha t}}\right) - \mathrm{erfc}\left(\frac{z}{2\sqrt{\alpha t}}\right)\mathrm{erfc}\left(\frac{x}{2\sqrt{\alpha t}}\right) + \frac{2(1-\alpha)}{\pi}\int_0^\infty [f_1(x,\rho,t) + f_2(x,\rho,t)]\sin(\rho z)\,d\rho \tag{17}$$

where,

$$f_1(x,\rho,t) = \frac{\rho}{B_1(B_1-B_2)} e^{\frac{x}{\sqrt{\alpha}}B_1 + B_1^2 t - \alpha\rho^2 t}\,\mathrm{erfc}\left(B_1\sqrt{t} + \frac{x}{2\sqrt{\alpha t}}\right) \tag{18}$$

$$f_2(x,\rho,t) = \frac{-\rho}{B_2(B_1-B_2)} e^{\frac{x}{\sqrt{\alpha}}B_2 + B_2^2 t - \alpha\rho^2 t}\,\mathrm{erfc}\left(B_2\sqrt{t} + \frac{x}{2\sqrt{\alpha t}}\right) \tag{19}$$

in which B_1 and B_2 are defined as:

$$B_1, B_2 = \frac{1}{2}\left[\frac{k}{\sqrt{\alpha}} \pm \sqrt{\Delta}\right] \qquad (\Delta > 0) \tag{20}$$

$$B_1, B_2 = \frac{1}{2}\left[\frac{k}{\sqrt{\alpha}} \pm i\sqrt{-\Delta}\right] \qquad (\Delta < 0) \tag{21}$$

with the determinant Δ defined by:

$$\Delta = \frac{k^2}{\alpha} + 4(\alpha - 1)\rho^2 \tag{22}$$

The expression for the pneumatic head in the fault zone may be readily obtained from Equation (17) by simply setting x = 0.

Case 2: Sinusoidal atmospheric pressure variation.

The procedure for solving the mathematical model with sinusoidal atmospheric pressure variation is very similar to the one described above and the expression for pneumatic head in the rock mass becomes:

$$\phi_r(x,z,t) = e^{-z\sqrt{\frac{\omega}{2\alpha}}}\sin\left(\omega t - z\sqrt{\frac{\omega}{2\alpha}}\right) + \frac{2\alpha\omega}{\pi}\int_0^\infty \frac{u e^{-\alpha u^2 t}\sin(uz)}{\omega^2 + \alpha^2 u^4}\,du + \omega\int_0^t \mathrm{erfc}\left(\frac{x}{2\sqrt{\alpha t}}\right)\left[1 - \mathrm{erfc}\left(\frac{z}{2\sqrt{\alpha t}}\right)\right]\cos[\omega(t-\tau)]\,d\tau + \frac{2(1-\alpha)\omega}{\pi}\int_0^\infty \sin(\rho z)\,d\rho \int_0^t [f_1(x,\rho,\tau) + f_2(x,\rho,\tau)]\cos[\omega(t-\tau)]\,d\tau \tag{23}$$

RESULTS AND DISCUSSION

In this section, we shall first present some of the results obtained from the evaluation of the solutions presented above. A discussion on the impact of various assumptions used in the setup of the mathematical model will then follow.

Figures 2 through 5 present some of the results obtained for case 1, i.e., step function atmospheric pressure variation. Figure 2 shows variation of dimensionless pneumatic head versus dimensionless depth within the fault zone for three values of dimensionless time and for a fixed ratio of rock to fault-zone permeability k=0.02. Figure 3 presents the variation of dimensionless pneumatic head with dimensionless distance from the fault-rock interface at a dimensionless depth of 20 and three values of dimensionless time. Corresponding values of pneumatic head in the absence of the fault are also shown. Figure 4 shows a snap shot of pneumatic head changes with distance away from the fault zone-rock contact for different levels of permeability ratio at the dimensionless depth of z = 20. To examine the effect of permeability contrast between the fault zone and the surrounding rocks, we have intentionally kept $\bar{p}/\mu_a n_a$ the same in the two regions.

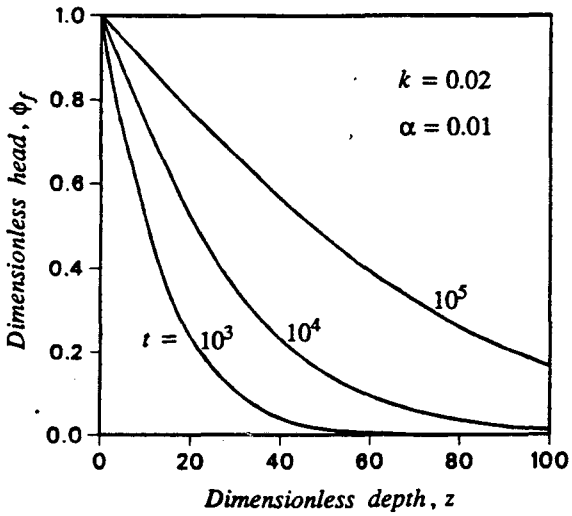

Figure 2. Variation of dimensionless pneumatic head versus dimensionless depth within the fault zone for three values of dimensionless time.

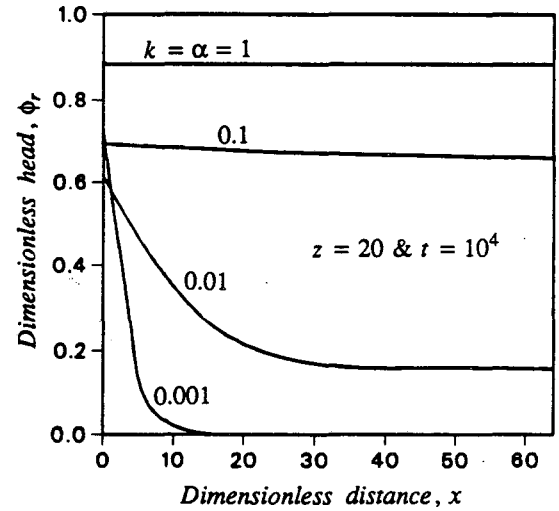

Figure 4. Effect of permeability contrast on dimensionless pneumatic head.

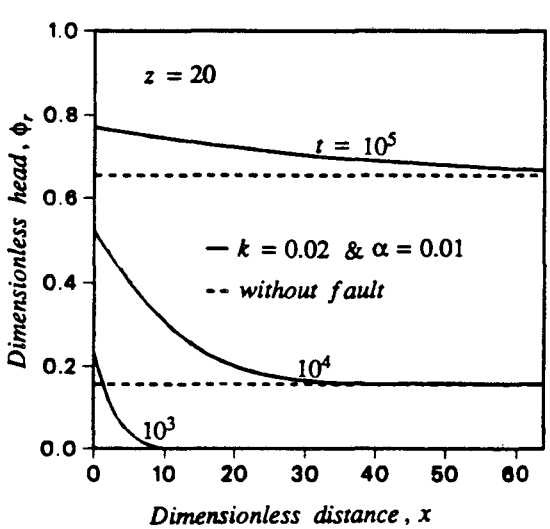

Figure 3. Variation of dimensionless pneumatic head versus dimensionless distance from the fault zone at z=20, for three values of dimensionless time.

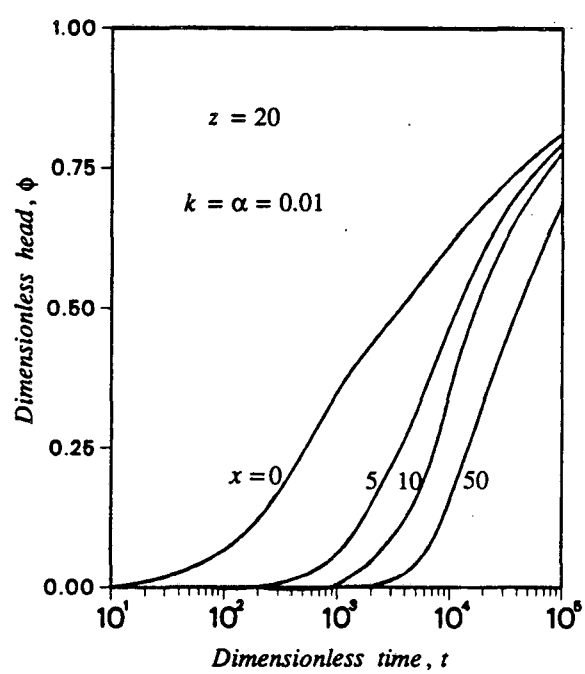

Figure 5. Dimensionless pneumatic head versus dimensionless time within the fault zone and three points within the rock mass, at the same depth, for z=20, and k=α=0.01.

As is apparent in Figure 4, at a given time, the gradient of pressure variation in the direction perpendicular to the fault increases with the permeability contrast (i.e., decreasing k). The gradient, however, decreases with time as shown in Figure 3. A close look at Figure 4 indicates that the curve for k=0.001 intersects the ones for k=0.01 and 0.1 at small values of x. This means that at that particular time some points in the vicinity of the fault zone may show higher pressure changes for k=0.001 than for larger k values. This can be explained by noting that under two conditions pressure changes at the fault-rock contact (i.e., x=0) are identical: (1) When permeability of the fault zone and the surrounding rock are equal and (2) when the permeability of the surrounding rock is zero. In both cases there is no flow across the contact. Case 1 corresponds to k=1 and case 2 to k=0. When permeability of the surrounding rock is less than that of the fault-zone, since there is flux from the fault toward the rock, at a given depth and time pressure change in the fault zone becomes smaller. That is why ϕ_r at x=0 and for k=0.1 and 0.01 become smaller than for k=1. However, when the rock permeability becomes very small, flux into the rock mass tends to diminish and as a result pressure change in the fault increases again.

Figure 5 presents time variation of pneumatic head within the fault zone and at points away from the fault at the depth corresponding to z=20 and permeability ratio k= 0.01.

Figures 6 and 7 present results obtained from evaluation of the solution for case 2 (sinusoidal atmospheric pressure variation). Figure 6 shows time variation of pneumatic head in the fault zone at three different

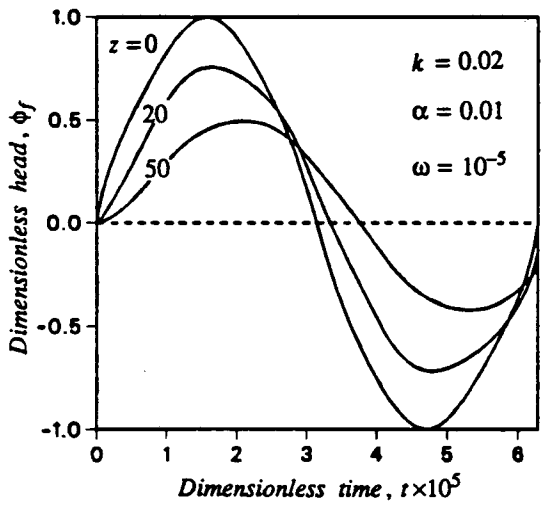

Figure 6. Dimensionless head versus dimensionless time in the fault zone at three different dimensionless depths.

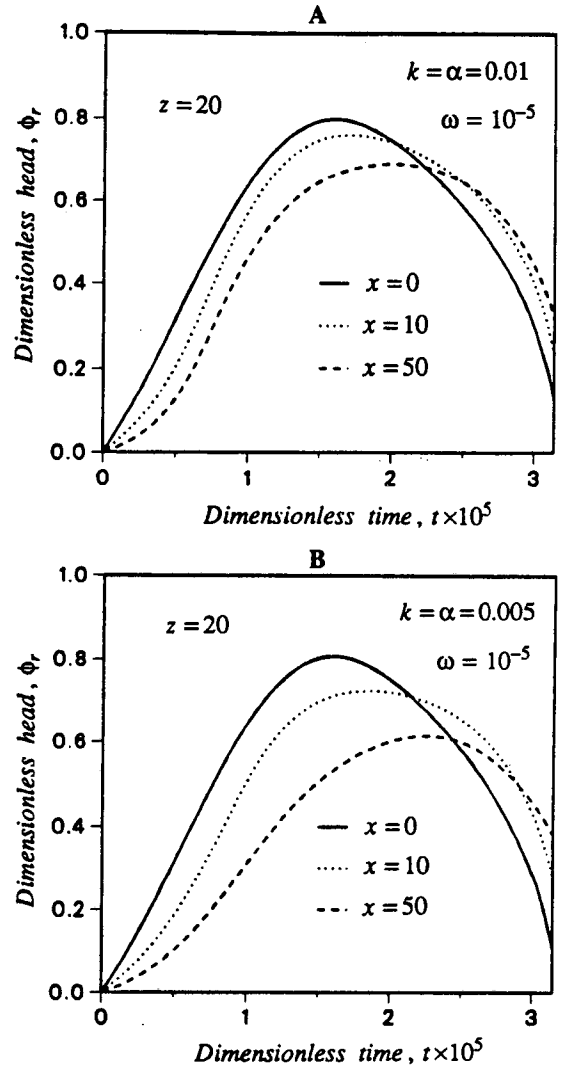

Figure 7. Time variation of pneumatic head within the fault zone and two other points away from the fault at the same depth, for z=20,and (A) k= α=0.01,(B) k=α=0.05.

depths for a permeability ratio k= 0.02. Figure 7A illustrates time variation of pneumatic head within the fault zone and at other points away from the fault at the same depth, for z=20 and k=0.01. Figure 7B shows results for the same set of parameters except for permeability ratio of 0.005. Note that when the permeability of the rock adjacent to the fault zone is significantly less than that of the fault zone, points located away from the fault will experience a smaller amplitude of pressure changes. The farther the points the smaller are the amplitudes. Furthermore, there is also a phase lag in the observed pressure changes. The farther the point from the fault the larger is the lag in the observed pressure changes. Such phenomenon seems to magnify when the permeability contrast increases (i.e., k decreases).

Examination of Figures 4, 5 and 7 reveals that when the contrast between permeability of the fault zone and surrounding rock is significant, the spatial pressure variations in the vicinity of the fault zone could be large enough to lend itself to be measured by conventional instruments. Therefore, air pressure data from isolated intervals in horizontal or inclined boreholes drilled through a fault zone may be analyzed to obtain the permeability ratio between the fault zone and surrounding rocks.

In the setup of the mathematical model certain assumptions were used. The validity and impact of these assumptions on the solutions will be discussed next.

To substitute Equation (2) for (1) we assumed that pneumatic head varies only slightly from its mean value. According to Weeks[1], pneumatic head changes are generally less than one percent of its mean value and thus the magnitude of error due to this assumption is within half a percent. Another assumption used in our development was that the effect of moisture content variation with time on the air permeability of the medium was insignificant. Although moisture content may change with time, such variations over the short time period needed for completing the test are not expected to be significant. In fact, measurement of pressure at various times, leading to different effective air permeabilities may be used to determine time variation of moisture content.

Furthermore, we assumed that flow in the fault zone is one dimensional, meaning that the equipotentials are essentially horizontal. The impact of this assumption on the accuracy of the solution may be evaluated with the help of numerical simulation. To do that, we first compared the results of our new analytical solutions with those obtained from the simulation of a well established code called TRUMP .[3] Figure 8 shows the comparison of results obtained by using these two approaches for a set of dimensionless parameters indicated in the figure and for both types of boundary conditions. As is clear from this figure, the agreement of two approaches is quite satisfactory. Then, TRUMP was used to simulate a model that allowed 2-D flow in both fault zone and the surrounding rocks. The results of this study revealed that except for very small values of time and small permeability contrasts, the assumption of one dimensional flow in the fault zone is quite reasonable. Figure 9 shows the distribution of pneumatic head in the system at a given depth and two values of time for a very small permeability contrast (k=0.5). It is clear that except for very small values of time and even for small permeability contrasts, equipotentials in the fault zone are essentially horizontal.

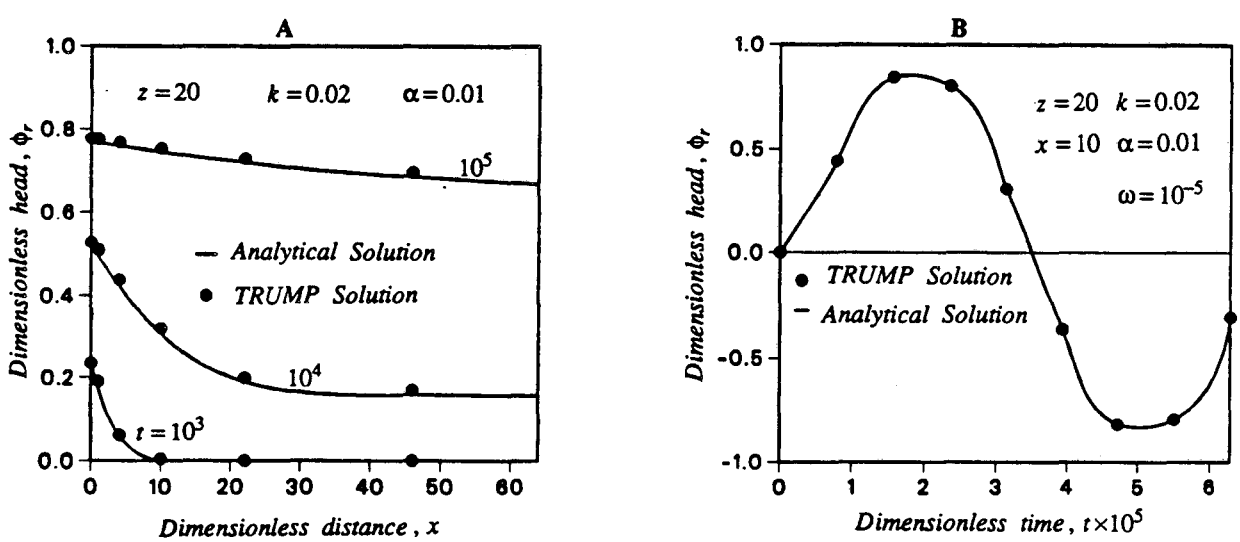

Figure 8. Comparison of present analytical solutions with numerical code TRUMP[3], (A) step function solution, and (B) sinusoidal solution.

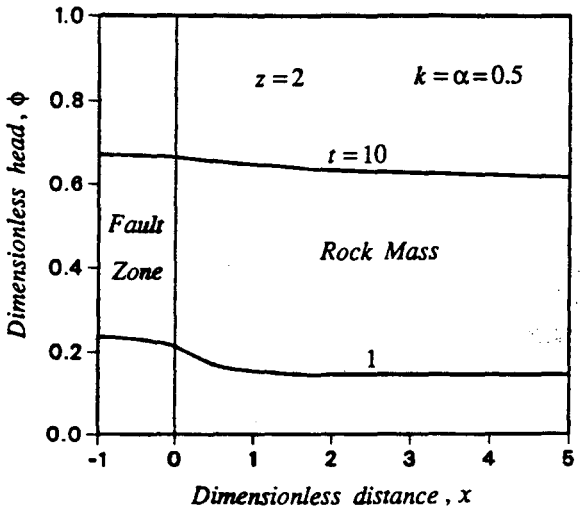

Figure 9. Distribution of pneumatic head in the system at z=2 and three values of time.

CONCLUSION

A series of new analytical solutions has been developed that predict transient pressure changes in the vicinity of major potentially highly conductive geologic features at depth due to barometric pressure variations at the land surface. Two of these solutions, one using step function and the other sinusoidal barometric pressure changes were presented. The results obtained from the evaluation of these solutions suggest that when the permeability of such features is at least an order of magnitude larger than that of the surrounding rocks, measurement of air pressure changes within isolated intervals in a horizontal or inclined borehole drilled through the fault zone may be used to estimate the ratio of permeability between the two media.

ACKNOWLEDGMENTS

The authors thank Marcelo Lippmann and Chin Fu Tsang for reviewing this manuscript. This work was sponsored by the Director, Office of Civilian Radioactive Waste Management, Office of Facilities Siting and Development, Siting and Facilities Technology Division of the U.S. Department of Energy Under Contract No. DE-AC03-76SF00098.

REFERENCES

1. E. P. WEEKS, "Field Determination of Vertical Permeability to Air in the Unsaturated Zone," *U.S. Geological Survey Professional Paper 1051*, (1978).
2. L. J. KLINKENBERG, "The Permeability of Porous Media to Liquids and Gases," *Amer Petroleum Inst. Drilling and Production Practice*, (1941).
3. A. L. EDWARDS, "TRUMP: A Computer Program for Transient and Steady State Temperature Distribution in Multidimensional Systems," *UCRL-14754, Lawrence Livermore Laboratory*, (1972).

LAWRENCE BERKELEY LABORATORY
TECHNICAL INFORMATION DEPARTMENT
1 CYCLOTRON ROAD
BERKELEY, CALIFORNIA 94720